biomass

MDPI

Article

Influence of Bran and Peat Binder Components on the Pyrolysis Products of Agricultural Residue-Based Biomass Pellets

Maryna Zhylina [1,2], Kristine Lazdovica [3], Mariia Shved [4], Denis Miroshnichenko [5,6,*], Andrei Shishkin [7] and Jurijs Ozolins [1]

1 Faculty of Natural Sciences and Technology, Institute of Biomaterials and Bioengineering, Riga Technical University, Paula Valdena Street 3, K-1, LV-1048 Riga, Latvia; maryna.zhylina@rtu.lv (M.Z.); jurijs.ozolins@rtu.lv (J.O.)
2 Institute of Agricultural Resources and Economics, Stende Researh Centre, Dizzemes, Dizstende, Libagu parish, LV-3258 Talsu County, Latvia
3 Faculty of Natural Sciences and Technology, Institute of Chemistry and Chemical Technology, Riga Technical University, LV-1048 Riga, Latvia; kristine.lazdovica@rtu.lv
4 The Department of Information Security, Lviv Polytechnic National University, 12 Bandera Street, 79013 Lviv, Ukraine; mari4ka.ved@ukr.net
5 Department of Oil, Gas and Solid Fuel Processing Technology, National Technical University Kharkiv Polytechnic Institute, 2, Kyrpychova Str., 61002 Kharkiv, Ukraine
6 Coal Department, State Enterprise Ukrainian State Research Institute for Carbochemistry (UKHIN), 7 Vesnina Str., 61023 Kharkiv, Ukraine
7 Faculty of Natural Sciences and Technology, Institute of Physics and Materials Science, Riga Technical University, 3 P. Valdena Str., LV-1048 Riga, Latvia; andrei.shishkin@rtu.lv
* Correspondence: denys.miroshnychenko@khpi.edu.ua

Abstract

Agricultural residues represent an abundant lignocellulosic resource for the production of renewable fuels and value-added products through thermochemical conversion. In this study, the influence of bran and peat as organic and mineral-rich binder components on the pyrolysis behaviour and product distribution of biomass pellets was investigated. Wheat straw, barley straw, and oat husks were pelletized using barley bran or peat as binders and analysed by thermogravimetric analysis coupled with Fourier-transform infrared spectroscopy (TGA-FTIR). The thermal degradation behaviour, product yields, evolution profiles of non-condensable gases, and composition of condensable products were evaluated during pyrolysis at 700 °C. The results indicated that pelletization modified the thermal degradation pathways and product distribution through interactions between biomass and binder components. Bran-bonded pellets promoted the formation of bio-oil and oxygen-containing condensable compounds, with bio-oil yields reaching up to 45.2%, whereas peat-bonded pellets showed increased formation of non-condensable gases and solid residue. CO_2 and CO were the dominant gaseous products, while CH_4 formation mainly occurred at elevated temperatures in the passive pyrolysis region. The results indicate that binder composition plays an important role in controlling pyrolysis pathways and product distribution, providing opportunities for the optimization of agricultural residue-based pellets for bioenergy and circular bioeconomy applications.

Keywords: agricultural residues; biomass pellets; pyrolysis; TGA-FTIR; bio-oil; non-condensable gases; bran binder; peat binder; thermochemical conversion; circular bioeconomy

Check for updates

Academic Editor: Rocio Maceiras

Received: 26 May 2026
Revised: 29 June 2026
Accepted: 30 June 2026
Published: 31 August 2026

Copyright: © 2026 by the authors. Licensee MDPI, Basel, Switzerland. This article is an open access article distributed under the terms and conditions of the Creative Commons Attribution (CC BY) license.

1. Introduction

The thermochemical conversion of biomass into energy-dense fuel and value-added products has attracted increasing attention in response to the growing demand for sustainable energy sources and effective waste management strategies. Among thermochemical conversion technologies, pyrolysis—the thermal decomposition of organic materials in an oxygen-free environment—is widely regarded as a promising route for transforming biomass into solid char, liquid condensates, and non-condensable gases [1,2]. Biomass-based pellets, particularly those produced from agricultural residues, provide a compact and energy-efficient feedstock for pyrolysis, offering improved handling, greater uniformity, and more predictable thermal behaviour compared with raw or loose biomass [3,4].

Previous studies have shown that compacted biomass forms, such as pellets, can improve feedstock handling and process stability, while also influencing heat and mass transfer, conversion behaviour, and pyrolysis product distribution [5,6]. Granulation, often referred to as pelletization in biomass processing, is therefore an effective densification approach prior to pyrolysis, as it increases bulk and energy density, enhances feeding behaviour, and reduces storage and transportation requirements [7]. Bielecki et al. reported that densification mainly affected the composition of volatile pyrolysis products, including saturated and unsaturated hydrocarbons, carbonyl-containing compounds, alcohols, and phenols, through intensified volatile–char interactions during pyrolysis [8]. Similarly, Crowley et al. showed that pelletization of pine biomass produced a denser and less permeable feedstock, which converted more slowly during fast pyrolysis and resulted in higher residual char formation compared with non-pelletized pine biomass [9].

The selection of binder materials for biomass granulation is a critical factor influencing pellet quality, including density, mechanical strength, and durability [10]. Organic binders, such as starch- or flour-rich agro-processing by-products, are often used due to their availability, binding capacity, and compatibility with lignocellulosic matrices [11]. In contrast, inorganic or mineral-rich additives may modify ash composition and influence thermal degradation pathways during pyrolysis [12]. However, limited research has been conducted on the pyrolysis performance of agricultural-residue-based pellets formulated with different binder components, particularly regarding how organic and mineral-rich binders affect thermal conversion behaviour, product distribution, and material properties.

Latvia generates substantial amounts of agricultural residues, including straw, husks, and grain-processing by-products such as bran, which represent promising feedstocks for thermochemical conversion. In addition, peat is a locally available mineral-rich material that may influence biomass pellet properties and pyrolysis behaviour [13,14].

Although agricultural residues and peat are individually recognized as relevant feedstocks or additives for thermochemical conversion, their combined use in biomass granule formulations remains insufficiently explored. In particular, limited information is available on how organic binder components such as bran and mineral-rich components such as peat affect granule properties, thermal degradation behaviour, and the distribution of pyrolysis products. Addressing this gap is particularly relevant for regions such as Latvia, where both agricultural by-products and peat resources are locally available.

Previous studies have investigated the pyrolysis of pelletized biomass and the use of individual additives; however, these studies have mainly focused on pellet quality, conversion efficiency, or overall product yields. A systematic comparison of chemically different binder types under identical pyrolysis conditions is still lacking. In particular, the mechanisms by which organic and mineral-rich binders modify thermal degradation pathways, volatile evolution, and the distribution of gaseous and condensable products have not been clearly established.

https://doi.org/10.3390/biomass6050068

The composition of non-condensable gases and condensable vapours is particularly important for evaluating the potential utilization of pyrolysis products as fuels, chemical intermediates, or precursors for further upgrading. Pyrolysis gas typically contains CO, CO_2, H_2, CH_4 and light hydrocarbons, and its composition strongly affects its potential energetic value and further use as a fuel or upgraded gas product [15,16]. Similarly, the chemical profile of condensable vapours and derived bio-oil provides insight into the formation of oxygenated compounds, phenolics, hydrocarbons, and other compounds relevant for fuel and chemical applications [17].

In the present study, barley bran and peat were selected as binder components because of their distinct physicochemical properties and expected influence on thermal decomposition processes. Barley bran contains starch, proteins, and other readily degradable organic compounds that may promote volatile release and affect the formation of condensable products during pyrolysis. In contrast, peat is rich in humic substances and mineral constituents, which may influence char formation, gas evolution, and secondary thermal reactions. In addition, barley bran exhibits good natural binding properties, enabling the production of durable pellets while maintaining a high proportion of agricultural biomass in the final product. Owing to their contrasting chemical compositions and thermal degradation characteristics, these materials provide a suitable basis for evaluating the influence of organic and mineral-rich binders on pyrolysis behaviour and product distribution.

To the best of our knowledge, this is the first study to systematically compare bran and peat as representative organic and mineral-rich binders under identical pyrolysis conditions using TGA–FTIR analysis. Beyond comparing product yields, this work provides mechanistic insight into how binder chemistry influences thermal degradation pathways, volatile evolution, and the formation of gaseous and condensable products in agricultural residue-based biomass pellets.

Therefore, the aim of this study was to investigate the influence of bran and peat binder components on the thermal degradation behaviour, volatile evolution, and product distribution of agricultural residue-based biomass pellets using TGA–FTIR analysis.

2. Materials and Methods

2.1. Physicochemical Properties of the Raw Materials

Wheat straw and barley straw were collected in September 2024 from Dižstende, Talsi District, Latvia. Barley bran and oat husk were obtained from AS "Dobeles dzirnavnieks" in Dobele, Latvia, while ZTK low-type peat from Lielvārde, Latvia, was used as an additional binder component. Prior to granule preparation, the biomass samples were dried at 60 °C for 24 h in a UF 110 drying oven (Memmert GmbH + Co. KG, Schwabach, Germany). The proximate and compositional characteristics of the raw materials are summarized in Table 2.

Proximate analysis was performed to determine volatile matter, fixed carbon, ash content, and moisture content of the biomass samples. Volatile matter and fixed carbon were determined from thermogravimetric analysis data obtained using a STA 6000 thermogravimetric analyzer (PerkinElmer Inc., Waltham, MA, USA) thermogravimetric analyzer, while fixed carbon was calculated by difference. Ash content was determined in a muffle furnace HTC 03/16 muffle furnace (Nabertherm GmbH, Lilienthal, Germany) according to ISO 5984:2022 [18]. Approximately 2 g of each biomass sample was placed in porcelain crucibles and ashed at 550 °C for 4 h until constant mass was achieved. Moisture content was determined according to LVS EN ISO 712:2011 [19] by drying 5 g biomass samples in aluminum containers at 105–110 °C for 2 h in a laboratory drying oven UF 110 drying oven (Memmert GmbH + Co. KG, Schwabach, Germany). The samples were then cooled

in a desiccator for 30 min and weighed using an analytical balance ABJ 220-4M analytical balance (KERN & SOHN GmbH, Balingen, Germany) [20].

Cellulose content was determined after Soxhlet extraction of biomass with ethanol-benzene (1:1) and subsequent mercerisation. Approximately 0.5 g of sample was treated with chilled 25% KOH, washed to neutrality, and further hydrolysed with an ethanol-nitric acid mixture (4:1) under reflux for 1.5 h. The resulting precipitate was filtered, washed with hot ethanol, dried at 105 °C to constantly weighed. Cellulose content was calculated as:

$$\boldsymbol{CEL}(\%) = \frac{\boldsymbol{B} - \boldsymbol{A}}{\boldsymbol{G_w}\left(\mathbf{1} - \frac{\boldsymbol{W_r}}{\mathbf{100}}\right)} \times \mathbf{100}, \quad (1)$$

where $\boldsymbol{A}$ is the filter mass (g), $\boldsymbol{B}$ is the filter + cellulose mass (g), $\boldsymbol{G_w}$ is the oven-dry biomass mass (g), $\boldsymbol{W_r}$—relative moisture (%).

Approximately 1 g of extracted dry biomass was hydrolyzed with 72% H_2SO_4 (Chempur, Piekary Śląskie, Poland), diluted, refluxed for 1 h, filtered, washed to neutrality and the residue was dried at 105 °C to constant weight. Lignin content was quantified by the Klason method. The lignin content in the analysed sample was calculated using the following formula:

$$\boldsymbol{L}(\%) = \frac{\boldsymbol{B} - \boldsymbol{C}}{\boldsymbol{G_w}\left(\mathbf{1} - \frac{\boldsymbol{W_r}}{\mathbf{100}}\right)} \times \mathbf{100}, \quad (2)$$

where $\boldsymbol{B}$ is the mass of the filter with lignin residue (g), $\boldsymbol{C}$ is the mass of the empty filter (g), $\boldsymbol{G_w}$ is the mass of the dry biomass sample (g), $\boldsymbol{W_r}$ is the relative moisture content of the biomass.

Biomass (3–5 g) was Soxhlet-extracted for 6–8 h with a 1:1 ethanol-benzene mixture (95% EtOH, Chempur, Piekary Śląskie, Poland). After cooling, the residue was weighed for further calculations.

The extractives content was determined as:

$$\boldsymbol{E}(\%) = \frac{\boldsymbol{G_0} - \boldsymbol{G_e}}{\boldsymbol{G_0}} \times \mathbf{100}, \quad (3)$$

where $\boldsymbol{G_0}$ is the oven-dry sample mass (g), $\boldsymbol{G_e}$ is the extracted sample mass (g).

It should be noted that the applied cellulose determination method, based on alkaline treatment (KOH) followed by ethanol–nitric acid hydrolysis, is not fully specific to cellulose and may include residual hemicellulose fractions, similarly to classical TAPPI-type procedures.

Holocellulose content was determined using the monoethanolamine method, based on selective delignification of biomass while preserving the carbohydrate fraction [21]. This approach is consistent with commonly used procedures for lignocellulosic compositional analysis. Approximately 2 g of oven-dry biomass was subjected to repeated chlorination and monoethanolamine treatment with intermediate washing steps until the sample became white. The residue was washed sequentially with ethanol, water, and ether, then dried at 103 °C to constant weight. The holocellulose content was calculated according to:

$$\boldsymbol{HOL}(\%) = \frac{\boldsymbol{B} - \boldsymbol{A}}{\boldsymbol{G_w}\left(\mathbf{1} - \frac{\boldsymbol{W_r}}{\mathbf{100}}\right)} \times \mathbf{100}, \quad (4)$$

where A is the mass of the empty filter (g), $\boldsymbol{B}$ is the mass of the filter with holocellulose (g), $\boldsymbol{G_w}$ is the oven-dry mass of biomass (g), $\boldsymbol{W_r}$ is the relative moisture (%).

Therefore, the calculated hemicellulose content, obtained as the difference between holocellulose and cellulose, should be considered as an approximate value and used primarily for comparative analysis between biomass types.

Elemental analysis for carbon (C^{daf}), hydrogen (H^{daf}), and nitrogen (N^{daf}) contents was performed using a Vario Macro CHNS elemental analyzer (Elementar Analysensysteme GmbH, Langenselbold, Germany) in accordance with CEN/TS 15104:2005 [22] instrumental methods. The total sulfur content was determined according to CEN 15289:2006 (Solid Biofuels: Determination of Total Content of Sulfur and Chlorine) [23]. Oxygen content was not determined directly but calculated by difference, assuming that the total elemental composition equals 100% on a dry ash-free (daf) basis. The oxygen content (O^{daf}) was calculated using Equation (5):

$$O^{daf} = 100 - C^{daf} - H^{daf} - N^{daf} - S^{daf}, \quad (5)$$

where C^{daf}, H^{daf}, N^{daf}, and S^{daf} represent the carbon, hydrogen, nitrogen, and sulfur contents, respectively, expressed on a dry ash-free basis [24].

2.2. Pellet Production

The biomass pellet production procedure followed the standard technological sequence described in a previous study [25,26], consisting of raw material pretreatment and preparation, homogenization of the pelletizing mixture, pellet formation, and pellet drying. The specific conditions applied at each stage may vary depending on the relative proportions and moisture content of the feedstock components, which are known to strongly influence the quality and physicochemical properties of the final pellets. In this study, biomass pelletization was carried out using a flat die pellet mill ZLSP 20.OB flat-die pellet mill (Anyang Best Complete Machinery Engineering Co., Ltd., Anyang, China). Six pellet formulations were prepared, including three peat-bonded and three bran-bonded pellet types, as summarized in Table 1.

Table 1. The composition of the pellets.

Sample	Composition
85WSP	85% Wheat straw + 15% peat
85BSP	85% Barley straw + 15% peat
85OHP	85% Oat husks + 15% peat
90WSB	90% Wheat straw + 10% barley bran
90BSB	90% Barley straw + 10% barley bran
90OHB	90% Oat husks + 10% barley bran

The binder contents used in this study were selected based on our previous optimization studies on biomass pellet production [25,27]. The primary objective was to maximize the proportion of agricultural biomass while maintaining sufficient pellet mechanical strength and durability for handling and thermochemical conversion. Barley bran exhibited high natural binding efficiency due to its starch and protein content; therefore, 10 wt.% was sufficient to produce durable pellets. In contrast, peat required 15 wt.% to achieve comparable pellet integrity because of its lower binding capacity. Lower binder contents resulted in mechanically weak and brittle pellets, whereas increasing the binder content reduced the biomass fraction without providing a significant improvement in pellet quality. Consequently, the selected formulations represent the optimum compromise between pellet quality and maximum biomass utilization.

2.3. TGA-FTIR Experiment

The thermogravimetric analyzer STA 6000 thermogravimetric analyzer (PerkinElmer Inc., Waltham, MA, USA) was interfaced with a Fourier-transform infrared spectrometer Spectrum 100 FTIR spectrometer (PerkinElmer Inc., Waltham, MA, USA) via a heated transfer line TL8000 heated transfer line (PerkinElmer Inc., Waltham, MA, USA) to enable simultaneous monitoring of mass loss and volatile product evolution during the thermal degradation of raw materials and pelletized samples. Both the transfer line and gas cell were maintained at a constant internal temperature of 230 °C to prevent condensation or adsorption of semi-volatile compounds. FTIR spectra were collected every 9 s across a spectral range of 4000–400 cm^{-1}, with a spectral resolution of 4 cm^{-1}. A time lag of approximately 90 s was observed between the TGA signal and the corresponding FTIR spectra. Since the transfer line configuration and operating conditions were identical for all experiments, this time lag remained constant throughout the study and did not affect the comparative evaluation of the thermal decomposition behaviour or the relative distribution of volatile products among the investigated samples. Dry biomass samples, weighing between 50 mg and 60 mg, were heated from 30 °C to 700 °C at a heating rate of 100 °C·min^{-1} under a nitrogen atmosphere flowing at 20 mL·min^{-1}, regulated by a mass flow controller. A heating rate of 100 °C·min^{-1} was selected to simulate rapid pyrolysis conditions and to ensure sufficient volatile evolution for TGA–FTIR analysis. Heating rate is known to influence the apparent decomposition temperatures, volatile evolution profiles, and product distribution because higher heating rates increase thermal lag and may enhance secondary cracking reactions. The same heating rate was applied to all samples to ensure a reliable comparative evaluation of the effect of binder composition on pyrolysis behaviour. Prior to analysis, the pellet samples were ground and homogenized to obtain representative material for TGA–FTIR measurements.

2.3.1. Volatile Matter (Non-Condensable Gases and Bio-Oil)

The yield volatile matter (VM) received in thermal pyrolysis is calculated based on mass changes during TG analysis according to Equation (6):

$$\boldsymbol{VM}(\%) = \frac{\boldsymbol{m_s - m_r}}{\boldsymbol{m_s}} \times \mathbf{100}, \quad (6)$$

where $\boldsymbol{m_s}$, $\boldsymbol{m_r}$—a mass of the sample and solid residue (fixed carbon, ash), g.

2.3.2. The Relative Yield of the Volatile Compounds

The standard output of the TGA-FTIR system consists of time-resolved infrared spectra, pre-programmed based on temperature, presented as three-dimensional (3D) absorbance stack plots that reflect the release of volatile compounds during thermal decomposition under an inert atmosphere.

Throughout the pyrolysis process, the collected TGA-FTIR data were compiled to generate absorbance profiles across the temperature range for each detected volatile component. In this study, the relative yield of each compound was determined by integrating the area under the corresponding absorbance-temperature curve (2D plot), following the methodology described in the literature [13,28].

The relative yield of each identified gaseous and condensable product was determined from the integrated area of the corresponding FTIR absorption band. Prior to integration, baseline correction was applied by subtracting the initial absorbance from the recorded spectra. Peak areas were calculated using the trapezoidal integration method over the selected temperature interval. Quantification was performed using previously established

calibration curves for the analysed compounds, and the obtained peak areas were converted into relative product yields.

2.3.3. Determination of Non-Condensable Gases

The TGA-FTIR technique was employed to quantify the concentrations of CO, CO_2, and CH_4 present in the volatile fraction generated during pyrolysis [29]. The amounts of non-condensable gases produced during the pyrolysis of the investigated raw materials and pellet formulations were calculated using Equation (7):

$$\boldsymbol{Non.cond.gases}(\%) = \frac{\boldsymbol{m_{CO2} + m_{CO} + m_{CH4}}}{\boldsymbol{m_{biomass}}} \times \mathbf{100}, \quad (7)$$

where $\boldsymbol{m_{biomass}}$, $\boldsymbol{m_{co2}}$, $\boldsymbol{m_{co}}$, $\boldsymbol{m_{CH4}}$—a mass of CO, CO_2, CH_4, and biomass, mg.

2.3.4. Determination of Bio-Oil

The amount of bio-oil obtained in the pyrolysis process calculated according to Equation (8):

$$\boldsymbol{Bio\text{-}oil}, (\%) = \boldsymbol{VM} - \boldsymbol{Non.cond.gases}, \quad (8)$$

where: ***VM***—volatile matter content (wt.%); ***Non-cond. gases***—yield of non-condensable gases (wt.%).

The bio-oil yield was estimated indirectly as the difference between the volatile matter yield and the yield of non-condensable gases. This calculation was used to enable a comparative evaluation of the investigated samples under identical experimental conditions. It assumes complete conversion of the volatile fraction into condensable and non-condensable products and does not account for possible experimental losses or incomplete recovery of volatile compounds. Therefore, the calculated bio-oil yield should be interpreted as a comparative rather than an absolute value.

2.3.5. Determination of Solid Residue Yield

The yield of the solid residue obtained after pyrolysis was determined from the residual mass recorded at the end of the TG experiment (700 °C) according to Equation (9):

$$\boldsymbol{Charyield}, (\%) = \mathbf{100} - \boldsymbol{VM}, \quad (9)$$

2.3.6. Determination of Aromatic Hydrocarbons and Olefins

Toluene (99.8%, Sigma-Aldrich, St. Louis, MO, USA) was used as standards and calibration materials for the quantification of monocyclic aromatic hydrocarbon. For olefin quantification, 1 hexadecene (≥99%, Sigma-Aldrich, St. Louis, MO, USA) was employed as the standard and calibration reference. The TGA-FTIR technique was utilized to determine the concentrations of monocyclic aromatic hydrocarbons and olefins present in the volatile fraction released during pyrolysis. The yield of hydrocarbons (i.e., monocyclic aromatic hydrocarbons and olefins) obtained during the pyrolysis of the investigated samples was calculated according to Equation (10):

$$\boldsymbol{Hydrocarbons}(\%) = \frac{\boldsymbol{m_{toluene} + m_{olefins}}}{\boldsymbol{m_{biomass}}} \times \mathbf{100}, \quad (10)$$

where $\boldsymbol{m_{biomass}}$, $\boldsymbol{m_{toluene}}$, $\boldsymbol{m_{olefins}}$—mass of toluene, xylene, olefins, and biomass, mg.

Toluene and 1-hexadecene were selected as representative calibration compounds for monocyclic aromatic hydrocarbons and olefins, respectively. The obtained calibration relationships were used to estimate the relative content of these compound groups from the integrated FTIR absorption bands. It should be noted that these compounds were used as

representative standards for comparative quantification and that the TGA–FTIR approach does not provide the compound-specific identification achievable by GC–MS.

2.3.7. Determination of Water from Pyrolysis

Calcium oxalate monohydrate (99%, Alfa Aesar, Haverhill, MA, USA) was employed as the standard and calibration material for water quantification. The TGA-FTIR technique was applied to determine the water content present in the volatile fraction generated during pyrolysis. Water content was quantified using a calibrated FTIR method to enable simultaneous analysis of all volatile products during pyrolysis. Although Karl Fischer titration is the reference method for absolute water determination, the FTIR approach was selected to provide a consistent comparative evaluation of water evolution under identical experimental conditions for all investigated samples.

2.3.8. Determination of Oxygen-Containing Compounds from Pyrolysis

The content of oxygen-containing compounds (%) was calculated using the following equation:

$$\boldsymbol{Oxygen\text{-}containingcompounds}, (\%) = \boldsymbol{Biooil} - \boldsymbol{water} - \boldsymbol{hydrocarbons}, \quad (11)$$

where ***Organic represents*** the total content of organic compounds (%), while ***Olefins*** and ***Toluene*** correspond to the respective compound groups (%) determined by analytical methods.

It should be noted that the applied TGA–FTIR methodology provides quantitative information only for the selected calibrated compound groups investigated in this study. Biomass pyrolysis vapours and bio-oils are known to contain numerous additional compounds, including phenolics, aldehydes, ketones, carboxylic acids, furans, and nitrogen-containing species, which cannot be comprehensively identified or quantified using FTIR alone. A detailed molecular characterization of these compounds would require complementary techniques such as GC–MS.

3. Results and Discussion

The reported values represent average experimental results obtained under identical experimental conditions. The original replicate datasets were unavailable at the time of manuscript revision; therefore, statistical parameters (standard deviations and error bars) could not be calculated retrospectively. Consequently, the quantitative results should be interpreted primarily as comparative trends rather than statistically validated differences. Accordingly, the discussion focuses on overall trends observed among the investigated samples rather than on small quantitative differences between individual formulations.

3.1. Characterization of Raw Materials

Table 2 summarizes the proximate, ultimate, and compositional properties of the raw lignocellulosic biomass samples investigated in this study.

The investigated biomass samples exhibited distinct differences in their chemical composition and fuel-related properties. Oat husks indicated the highest volatile matter content (71.3 wt.%) and cellulose content (35.2 wt.%), whereas barley straw contained the highest fixed carbon content (29.7 wt.%). Wheat straw was characterized by the highest lignin content (22.4 wt.%), which may contribute to improved thermal stability during thermochemical conversion processes. The oxygen content of all samples remained relatively similar, ranging from 43.3 to 43.6 wt.%, indicating the lignocellulosic nature of the selected agricultural residues. These differences in composition are expected to influence the thermal degradation behavior and gaseous product formation during pyrolysis.

Table 2. Analytical results for the investigated biomass samples.

Biomass Samples	Proximate Analysis (wt.%)				Composition Analysis (wt.%)					Ultimate Analysis (wt.%)				
	Volatile Matter	Fixed Carbon	Ash Content	Relative Moisture	Cellulose	Lignin	Extractives	Holocellulose	Hemicellulose	Carbon	Hydrogen	Nitrogen	Sulfur	Oxygen
Wheat straw	69.2	26.7	4.1	6.2	42.7	22.4	2.5	71.1	28.4	47.6	6.2	0.8	0.02	43.3
Barley straw	65.4	29.7	4.9	6.5	46.6	20.5	2.1	72.5	25.9	46.7	6.1	0.8	0.10	43.3
Oat husks	71.3	24.8	3.9	6.8	39.2	20.5	1.4	74.5	35.2	47.3	6.4	0.8	0.05	43.6

3.2. Thermal Decomposition of Raw Materials and Pelletized Samples

The thermogravimetric (TG) and derivative thermogravimetric (DTG) curves of raw materials and pelletized samples pyrolysis from 30 to 700 °C at the heating rate of 100 °C·min^{-1} are presented in Figure 1. The characteristic points of the TG and DTG curves are summarised in Table 3.

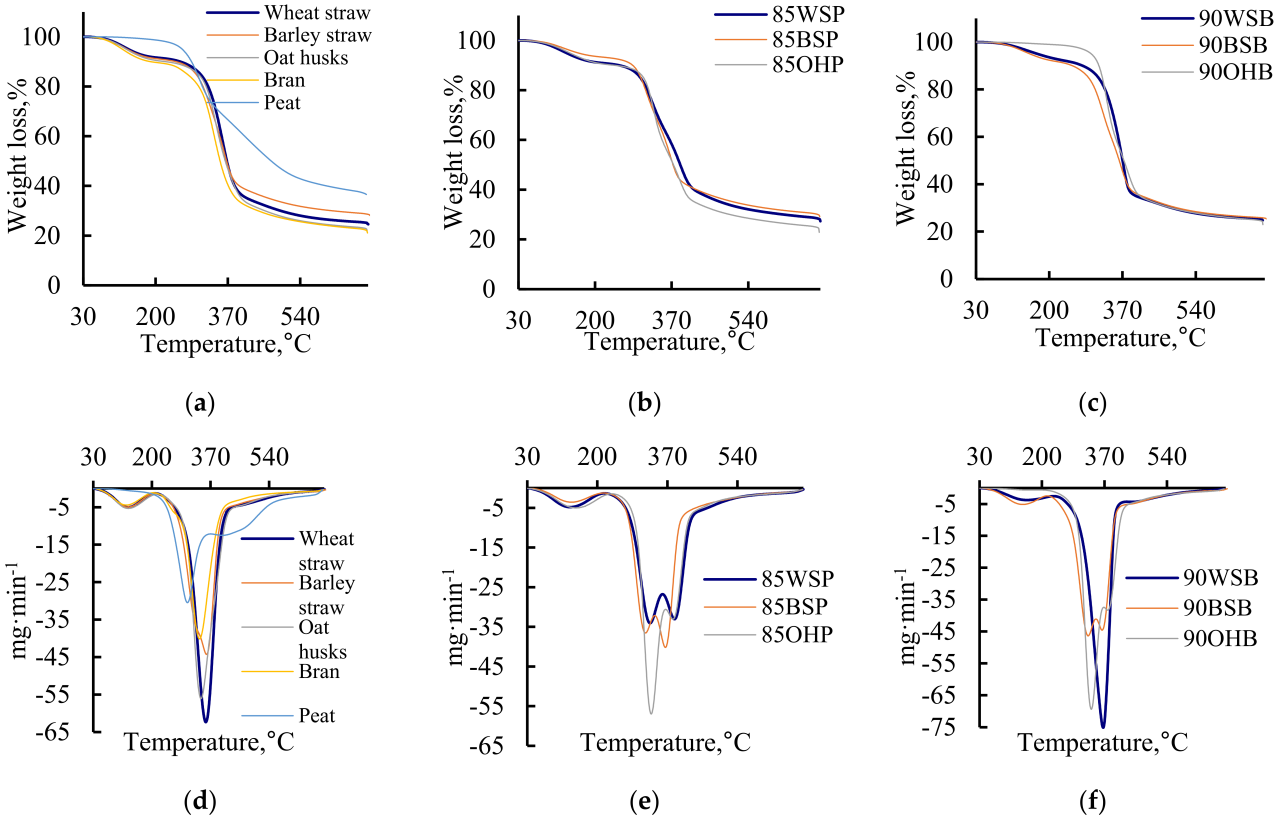


Figure 1. TG (**a**–**c**) and DTG (**d**–**f**) curves of raw materials and pelletized samples pyrolysis.

The thermal degradation of raw materials and pelletized samples occurred in three major weight loss steps: (I) dehydration, (II) degradation of organic components, and (III) charring of the residue. The first weight-loss step, corresponding to the removal of moisture and light components, occurred over a temperature range of 30–180 °C. Barley bran exhibited the highest moisture content among the raw materials at 9.5 wt.%, while wheat straw had the lowest at approximately 7.5 wt.%. Since peat can contain up to 80 wt.% moisture, it was dried before pyrolysis experiments, resulting in a negligible moisture content of approximately 1 wt.%. For pelletized samples using peat (85WSP, 85BSP, and

85OHP) or bran (90WSP, 90BSP, and 85OHP) as binders, the relative moisture content remains below 9.5 wt.%.

Table 3. The characteristic points of the TG and DTG curves in thermal pyrolysis.

Samples	Active Pyrolysis Zone			Passive Pyrolysis Zone
	T_i, °C	T_{max}, °C	T_f, °C	T_f^2, °C
Wheat straw	194	329	406	577
Barley straw	192	331	395	622
Oat husks	198	320	416	585
Barley bran	181	310	403	600
Peat	150	273 and 379	536	700
85WSP	203	300 and 360	415	640
85BSP	198	290 and 337	390	640
85OHP	220	305 and 358	414	635
90WSB	248	367	410	600
90BSB	235	325 and 367	410	600
90OHB	242	305 and 350	405	560

T_i—pyrolysis initial temperature; T_{max}, (DTG max)—where the rate of weight loss is maximum; T_f—the final temperature of the active pyrolysis zone; T_f^2—pyrolysis final temperature.

The main weight-loss step occurred over a wide temperature range from 190 °C to 520 °C and is associated with the degradation of the organic components of raw materials and pelletized samples, representing the active pyrolysis zone. This step is ascribed to a series of reactions involving dehydration, decarboxylation, decarbonylation, fragmentation, and rearrangement. Among all the raw materials examined, peat exhibits the lowest thermal stability. Its thermal degradation commences at 150 °C, a property attributed to its high hemicellulose and fulvic acid content. As a result, pelletized samples utilising peat as a binder exhibit lower thermal stability than those utilising bran.

In contrast to raw materials, the inflection points during the active pyrolysis step exhibit significant changes in pelletized samples. The observed phenomenon may result from interactions between biomass and binder components during thermal degradation. When multiple raw materials, including polysaccharides (hemicellulose), proteins, lignin, and humic substances, are combined, their co-pyrolysis behaviour cannot be predicted by the simple additive effects of individual components. These interactions modify degradation pathways, reaction rates, and product distributions [30].

All pelletized samples utilising peat as a binder exhibit two inflection points in the active pyrolysis zone. In the case of peat, these inflection points occur at 273 °C and 379 °C. The first inflection point corresponds to the thermal degradation of hemicellulose and is partially related to the decomposition of fulvic and humic acids. The second inflection point is attributed to the thermal degradation of lignin and the complete decomposition of fulvic and humic acids. Although the peat content in the pellets is relatively low (15 wt.%), the first inflection point increases and the second inflection point decreases for all pelletized samples compared to pure peat. The thermal stability of less stable components is altered through interactions with more stable components, resulting in a modified overall thermal stability of the pellets.

Scientifically interesting results are associated with the use of bran as a binder. All lignocellulosic raw materials in the active pyrolysis zone exhibit a single inflection point. However, for bran, this inflection point does occur at a lower temperature (310 °C) compared to straw (~330 °C) and husks (320 °C). This difference can be attributed to the presence of proteins and starch in bran, which degrade at slightly lower temperatures than cellulose and lignin, the primary constituents of straw and husks. In contrast, the active

pyrolysis zone in pelletized samples exhibits distinct characteristics. Although bran is present as a binder at only 10 wt.%, it exerts a substantial influence on the DTG characteristics. The 90BSB and 90OHB samples display two inflection points in the active pyrolysis zone, whereas the 90WSB sample exhibits only one. Furthermore, the second inflection points of 90BSB and 90OHB, as well as the sole inflection point of 90WSB, tend to occur at higher temperatures than those of the raw materials. These significant changes are likely due to protein complicated interactions with other chemical components in the pelletized samples during pyrolysis. Thermochemical degradation of protein occurs across a broad temperature range, from 250 °C to 1000 °C [13]. In pelletized samples, the first inflection point is likely associated with the thermal degradation of hemicellulose and partial protein degradation. The second inflection point appears to correspond to the thermal degradation of cellulose, lignin, and additional proteins.

During pyrolysis, proteins undergo deamination, decarboxylation, and fragmentation reactions over a broad temperature range, producing ammonia, amines, nitriles, pyrroles, and other nitrogen-containing intermediates. These reactive species may participate in secondary reactions with carbohydrate- and lignin-derived volatiles, thereby modifying volatile evolution profiles and thermal degradation pathways. In addition, Maillard-type reactions between proteins and reducing sugars may contribute to the formation of more thermally stable intermediates and carbonaceous structures, influencing both volatile composition and char formation [31].

The final temperature of the active pyrolysis zone does not exceed 420 °C for all lignocellulosic biomasses and pelletized samples, whereas it reaches 536 °C for peat. The final weight loss step observed between approximately 420 and 700 °C corresponds to the passive pyrolysis zone, in which the remaining carbonaceous residue undergoes slow thermal decomposition and carbonization, resulting in further char formation and the release of small amounts of non-condensable gases.

Thermal degradation yields the highest volatile matter from barley bran (69.4 wt.%), oat husks (68.9 wt.%), and wheat straw (67.9 wt.%). Although peat initiates decomposition earlier and proceeds over a wide temperature range, it yields a substantial amount of solid residue (36.5 wt.%). Pelletized samples that use peat as a binder exhibit volatile matter levels during thermal destruction that are comparable to those of the raw material without a binder. However, 85WSP shows a slightly higher solid residue (27.3 wt.%) than wheat straw (24.6 wt.%). The use of bran as a binder has minimal impact on the volatile matter content of pelletized samples during thermal degradation. For all pellets, the solid residue either decreased slightly or remained unchanged compared to the raw material.

The findings indicate that pelletization substantially modifies the thermal degradation behaviour of lignocellulosic biomass because of interactions between biomass and binder components. Notably, incorporating bran as a binder, even at low concentrations, appears to modify pyrolysis pathways through protein-mediated interactions, thereby altering thermal stability.

3.3. Product Yields Obtained from Raw Materials and Pelletized Samples During Thermal Pyrolysis

Figure 2 presents the product yields obtained from dry raw materials and pelletized samples during thermal pyrolysis at 700 °C. The reported values represent the average experimental results and were used for the comparative evaluation of the investigated biomass samples under identical experimental conditions.

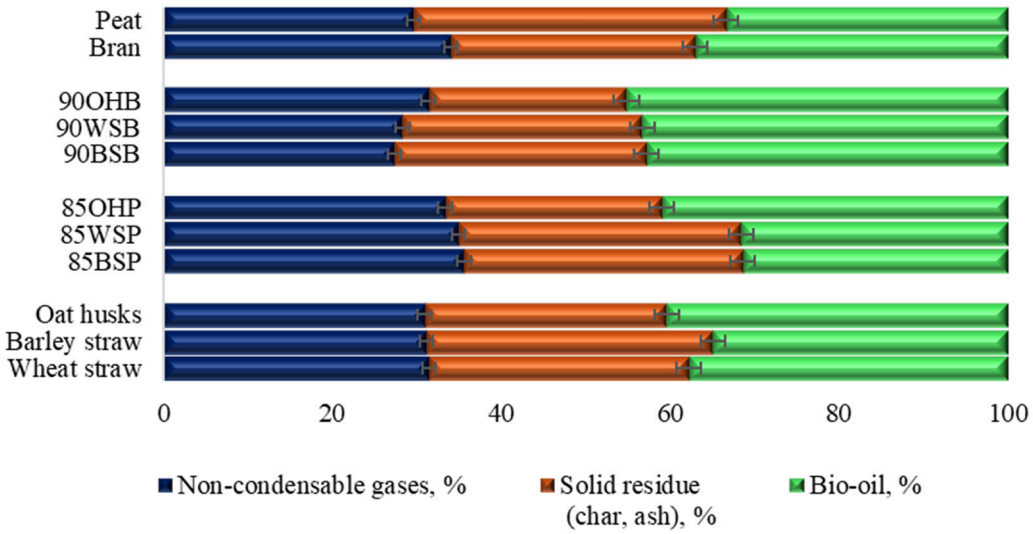


Figure 2. Product yields obtained from dry raw materials and pelletized samples during thermal pyrolysis at 700 °C. Values represent average experimental results.

Among the raw materials analysed, wheat bran produces the highest yield of non-condensable gases during pyrolysis (34.0%), whereas peat results in the lowest yield (approximately 29.6%). Peat also produces the lowest bio-oil yield (33.4%) and the largest amount of solid residue (37.1%). These results can be attributed to the more aromatic chemical structure of peat, which facilitates biochar formation during pyrolysis. Oat husks produce the highest bio-oil yield (40.4%), likely due to their elevated hemicellulose content and reduced lignin content.

Among the pelletized samples, 85OHP and 90OHB achieved the highest bio-oil yields of 41.0% and 45.2%, respectively. Notably, pelletized samples utilising bran as a binder exhibited higher bio-oil yields than both the raw materials and other pelletized samples. This suggests a specific interaction between the components during pyrolysis that favours the formation of the condensable fraction rather than the non-condensable fraction, which is the dominant pyrolysis product for wheat bran.

Although peat produces the lowest yield of non-condensable gases during pyrolysis, its use as a binder in pelletized samples increases the formation of non-condensable gases, reaching up to 35.6% in the case of 85BSP.

The chemical composition of binders influences the product distribution of lignocellulosic biomass during pyrolysis. Binders with higher protein content, interacting with lignocellulosic biomass components, tend to promote the formation of bio-oil. In contrast, binders with a more aromatic structure favour the formation of non-condensable gases. These differences can be attributed to the contrasting biochemical composition of the binder materials. Barley bran contains readily degradable polysaccharides, starch, and proteins, which promote volatile formation and increase the condensable product yield. In contrast, the humified aromatic structure and mineral constituents of peat favour dehydration and char-forming reactions, resulting in higher solid residue and gas production, in agreement with previous studies [16,32].

3.4. Composition and Evolution Profiles of Non-Condensable Gases from Raw Materials and Pelletized Samples During Thermal Pyrolysis

Composition of the non-condensable gases resulting from the raw materials and pelletized samples during thermal pyrolysis is shown in Figure 3.

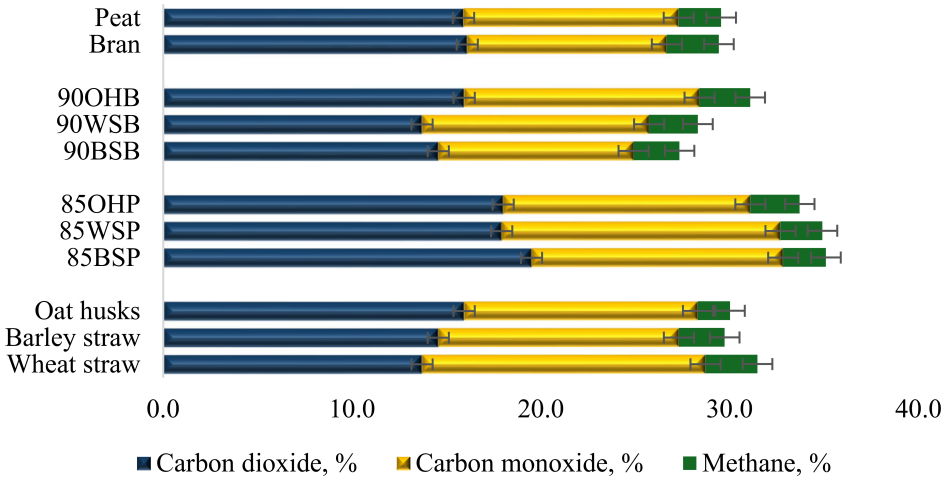


Figure 3. Composition of non-condensable gases from dry raw materials and pelletized samples during thermal pyrolysis at 700 °C temperature. Values represent average experimental results.

The non-condensable gas composition was dominated by CO_2 and CO in all analysed samples, while CH_4 represented only a minor fraction. The dominance of CO_2 and CO indicates that decarboxylation, decarbonylation, and secondary cracking reactions were the main contributors to gas formation during pyrolysis [16]. Raw biomass materials showed relatively similar gas profiles, although slight differences in CO_2, CO, and CH_4 contents may be related to variations in lignocellulosic composition and mineral matter.

Binder composition clearly affected the gas profile of the pelletized samples. Peat-bonded pellets showed comparatively higher total gas contributions and slightly enhanced CH_4 formation, which may be associated with the aromatic and humified structure of peat and its mineral constituents. In contrast, bran-bonded pellets showed substantial CO_2 and CO formation but comparatively lower CH_4 contents, consistent with the organic and oxygen-rich nature of bran. These results confirm that binder type influences the gas-forming pathways during pyrolysis and affects the distribution of non-condensable gas products.

CO_2 release was observed for all studied samples in both the active and passive pyrolysis regions, over approximately from 200 to 700 °C (Figure 4). A single dominant peak appeared in the active pyrolysis zone (around 350–420 °C). The highest CO_2 emissions occurred in biomass samples with peat as a binder. This indicates enhanced decomposition of oxygen-containing functional groups. The onset of CO_2 evolution occurred at the lowest temperature in peat (~190 °C) and the highest in bran (~255 °C), reflecting differences in thermal stability.

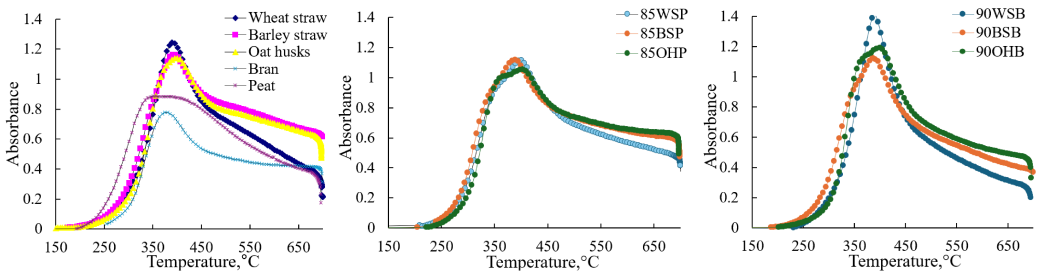


Figure 4. The evolution of CO_2 during thermal pyrolysis of raw materials and pelletized samples.

In the active pyrolysis region, CO_2 release is mainly associated with the decomposition of cellulose and hemicellulose. In the passive pyrolysis region (>450 °C), it is attributed to the gradual degradation of more stable aromatic structures. The extended

high-temperature tail in some samples suggests thermally resistant carbonaceous structures and secondary reactions.

CO release was observed for all investigated samples mainly within the active pyrolysis region, approximately between 250 and 450 °C (Figure 5). A dominant CO evolution peak appeared around 350–400 °C for both raw materials and pelletized samples. The highest CO emissions were detected for wheat straw and pelletized biomass samples containing peat as a binder. In contrast, peat exhibited a broader and less intensive CO release profile. CO formation during pyrolysis is primarily associated with the thermal degradation of oxygen-containing functional groups, including carbonyl, carboxyl, and ether structures originating from hemicellulose, cellulose, and partially lignin decomposition. The gradual decrease in CO release intensity above 450 °C indicates the depletion of thermally unstable oxygenated compounds. However, the extended high-temperature tail observed in pelletized samples suggests the contribution of secondary cracking reactions and the decomposition of more stable carbonaceous structures.

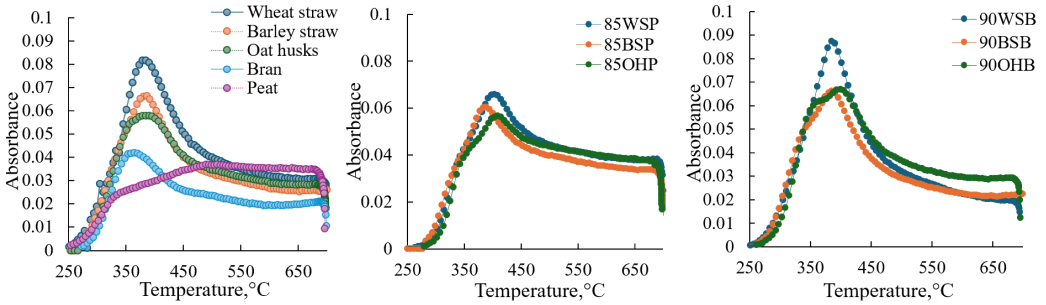


Figure 5. The evolution of CO during thermal pyrolysis of raw materials and pelletized samples.

CH_4 evolution was mainly observed in the passive pyrolysis region at temperatures above 400 °C (Figure 6). Unlike CO_2 and CO, methane formation occurred over a broader temperature range, with the maximum CH_4 release detected between approximately 550 and 680 °C. The highest methane emissions were observed for wheat straw and oat husk pellet samples, while bran-containing samples showed comparatively lower CH_4 evolution intensity.

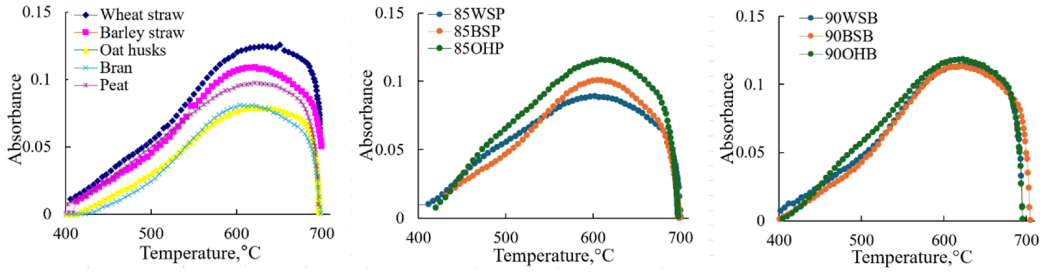


Figure 6. The evolution of CH_4 during thermal pyrolysis of raw materials and pelletized samples.

CH_4 formation is mainly related to the thermal decomposition of lignin-derived aromatic structures and secondary reactions occurring during high-temperature pyrolysis. The broad methane evolution profiles indicate gradual degradation of thermally stable carbonaceous components. Increased CH_4 release at elevated temperatures may also be associated with secondary tar cracking and methanation reactions. The higher CH_4 formation observed in some pelletized samples suggests enhanced secondary conversion reactions promoted by prolonged volatile residence time within the pellet structure.

The mineral constituents naturally present in peat, including alkali and alkaline-earth metals, may also influence pyrolysis reactions. These inorganic species have been reported

to promote dehydration, decarboxylation, and deoxygenation reactions while suppressing the formation of condensable oxygenated products. Consequently, a greater proportion of oxygen is released as CO_2, CO, and H_2O, accompanied by increased char formation [12].

3.5. Composition of Bio-Oil from Raw Materials and Pelletized Samples During Thermal Pyrolysis

The distribution of major compound groups in the condensable products (bio-oil) varied depending on the raw material and binder type (Figure 7). Oxygen-containing compounds were the dominant fraction in all analysed samples, indicating that cellulose, hemicellulose, lignin, and binder-derived oxygenated structures contributed substantially to the formation of condensable vapours. Among the raw biomass materials, oat husks and wheat straw showed the highest contents of oxygen-containing compounds, reaching 24.6% and 23.6%, respectively, whereas peat showed the highest value among the binder materials, at 21.3%. The hydrocarbon fraction remained comparatively low in all raw materials and binders, not exceeding 4.8%.

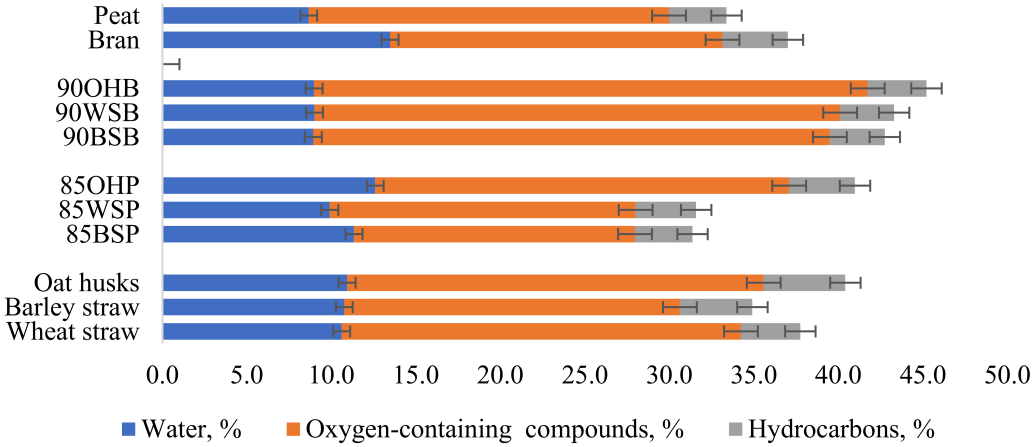


Figure 7. Composition of bio-oil from dry raw materials and pelletized samples during thermal pyrolysis at 700 °C temperature. Values represent average experimental results.

It should be noted that the detected water does not originate from the initial moisture content of the biomass, as all samples were dried prior to pyrolysis. Instead, it is mainly formed during thermal decomposition through dehydration reactions of cellulose, hemicellulose, lignin, and the organic constituents of the binder materials. Therefore, the water content reported in the condensable products represents reaction water generated during pyrolysis.

The binder composition influenced the condensable product profile of the pelletized samples. All bran-bonded pelletized samples showed a high proportion of oxygen-containing compounds in the condensable products (bio-oil), exceeding 30%, whereas the water content remained below 10%. This may be related to the organic and volatile-rich nature of bran, which can promote the formation of oxygen-rich condensable products during pyrolysis. In contrast, peat-bonded pelletized samples exhibited lower proportions of oxygen-containing compounds, ranging from 16 to 24%, while showing comparatively higher water contents, suggesting a different degradation pathway and a stronger contribution of dehydration reactions.

The differences observed between bran- and peat-bonded pellets can be related to the contrasting chemical compositions of the binder materials. Bran contains substantial amounts of organic constituents, including non-starch polysaccharides, starch, proteins, lipids, and minerals, which can readily decompose during pyrolysis and contribute to the formation of volatile products. In particular, polysaccharide-derived structures are known to generate oxygen-containing compounds during pyrolysis, while proteins can modify the

volatile product profile through the formation of nitrogen-containing species. Thus, the higher proportion of oxygen-containing compounds in bran-bonded pellets suggests that interactions between bran and lignocellulosic residues enhanced the release of oxygen-rich condensable products [33]. In contrast, peat-bonded pellets showed lower proportions of oxygen-containing organic compounds and higher water contents. This may be associated with the humified, more aromatic structure of peat and its mineral constituents, which can favour dehydration, char formation, and secondary deoxygenation reactions, leading to a greater release of oxygen as water and permanent gases rather than retention in the condensable organic fraction [34,35].

Besides their structural role, inorganic constituents in peat may exert a catalytic effect on pyrolysis reactions. Mineral species have been reported to accelerate dehydration, decarboxylation, and secondary deoxygenation reactions, thereby reducing the proportion of oxygenated condensable compounds while increasing the formation of permanent gases and solid carbonaceous residue. Although the catalytic contribution of individual mineral species was not investigated in the present study, the observed product distribution is consistent with these mechanisms reported in the literature [12].

The present results should therefore be interpreted as representing the relative distribution of the major calibrated compound groups rather than the complete chemical composition of the condensable fraction. Biomass-derived bio-oils are complex mixtures that typically contain phenolics, aldehydes, ketones, carboxylic acids, furans, and nitrogen-containing compounds originating from the thermal degradation of lignin, carbohydrates, and proteins. The applied TGA–FTIR methodology does not provide compound-specific identification of these species; therefore, complementary techniques such as GC–MS would be required for comprehensive molecular characterization.

From a practical perspective, the selection of binder materials should consider not only pyrolysis performance but also economic and environmental aspects. Barley bran is an abundant agricultural by-product generated during cereal processing and is widely available in grain-producing regions. Its use as a pellet binder represents a value-added utilization pathway consistent with circular bioeconomy principles while requiring only 10 wt.% binder to achieve satisfactory pellet quality. In contrast, peat provides favourable pellet strength and promotes the formation of char and gaseous products; however, peat is a slowly renewable resource, and its extraction may result in greenhouse gas emissions and ecosystem disturbance. Therefore, peat utilisation should be carefully evaluated according to regional regulations and sustainability objectives.

The pellet production technology applied in this study is compatible with conventional industrial pelletization systems and therefore can be readily implemented at a larger scale without substantial process modifications. Furthermore, binder selection may be adjusted according to the desired product distribution. Bran-containing pellets are more suitable when higher bio-oil yields are required, whereas peat-containing pellets may be advantageous when increased char production or combustible gas generation is preferred. Consequently, the proposed pellet formulations provide flexibility for different thermochemical conversion pathways depending on the intended industrial application.

The present results should be interpreted together with our previously published TG–DSC investigation of peat-bonded biomass pellets [24], which suggested that pelletization produced only minor changes in the thermal effects of decomposition. Consequently, the present TGA–FTIR study complements the previous thermal analysis by providing detailed information on volatile evolution and pyrolysis product distribution associated with different binder materials.

4. Conclusions

The present study suggests that pelletization and binder composition may influence the thermal degradation behaviour and pyrolysis product distribution of agricultural residue-based biomass pellets. TGA–FTIR analysis suggested that binder composition influenced the thermal decomposition pathways and evolution profiles of volatile products in lignocellulosic biomass pellets. Bran-bonded pellets promoted the formation of condensable products and oxygen-containing compounds, resulting in the highest bio-oil yield of 45.2% for the 90OHB sample. In contrast, peat-bonded pellets favoured the formation of non-condensable gases and solid residue due to the more aromatic and mineral-rich structure of peat. CO_2 and CO were identified as the dominant gaseous products during pyrolysis, while CH_4 evolution mainly occurred in the passive pyrolysis region at elevated temperatures. The results indicate that organic and mineral-rich binders influence pyrolysis through different degradation mechanisms. Bran enhanced the release of oxygen-rich condensable products, whereas peat promoted dehydration, char formation, and secondary deoxygenation reactions.

Overall, the findings demonstrate that appropriate binder selection provides a practical approach for tailoring pyrolysis product distribution according to specific industrial objectives. Barley bran appears particularly attractive for circular bioeconomy applications because it is an agricultural by-product that enhances bio-oil production, whereas peat-containing formulations may be more suitable where increased char production is required, provided that their environmental implications are carefully considered.

Author Contributions: Conceptualization, M.Z. and K.L.; methodology, M.Z. and D.M.; investigation, M.Z., K.L. and M.S.; data curation, M.Z.; writing—original draft preparation, M.Z., K.L. and A.S.; writing—review and editing, A.S. and J.O.; supervision, D.M. and J.O. All authors have read and agreed to the published version of the manuscript.

Funding: This activity/work has been supported by the EU Recovery and Resilience Facility within Project No 5.2.1.1.i.0/2/24/I/CFLA/003 "Implementation of consolidation and management changes at Riga Technical University, Liepaja University, Rezekne Academy of Technology, Latvian Maritime Academy and Liepaja Maritime College for the progress towards excellence in higher education, science and innovation" academic career doctoral grant (ID 1024). The paper was elaborated within the scope of the project: 'Utilization of agricultural residues' Institute of Agricultural Resources and Economics.

Data Availability Statement: The raw data supporting the conclusions of this article will be made available by the authors on request.

Conflicts of Interest: The authors declare no conflicts of interest.

References

1. Mullen, C.A.; Boateng, A.A. Catalytic Pyrolysis-GC/MS of Lignin from Several Sources. *Fuel Process. Technol.* **2010**, *91*, 1446–1458. [CrossRef]
2. Bridgwater, A.V. Review of Fast Pyrolysis of Biomass and Product Upgrading. *Biomass Bioenergy* **2012**, *38*, 68–94. [CrossRef]
3. Saidur, R.; Abdelaziz, E.A.; Demirbas, A.; Hossain, M.S.; Mekhilef, S. A Review on Biomass as a Fuel for Boilers. *Renew. Sustain. Energy Rev.* **2011**, *15*, 2262–2289. [CrossRef]
4. Eling, J.; Okot, D.K.; Menya, E.; Atim, M.R. Densification of Raw and Torrefied Biomass: A Review. *Biomass Bioenergy* **2024**, *184*, 107210. [CrossRef]
5. Mani, S.; Tabil, L.G.; Sokhansanj, S. Grinding Performance and Physical Properties of Wheat and Barley Straws, Corn Stover and Switchgrass. *Biomass Bioenergy* **2004**, *27*, 339–352. [CrossRef]
6. Saldarriaga, J.F.; Aguado, R.; Pablos, A.; Amutio, M.; Olazar, M.; Bilbao, J. Fast Characterization of Biomass Fuels by Thermogravimetric Analysis (TGA). *Fuel* **2015**, *140*, 744–751. [CrossRef]
7. Dhyani, V.; Bhaskar, T. Pyrolysis of Biomass. In *Biomass, Biofuels, Biochemicals: Biofuels: Alternative Feedstocks and Conversion Processes for the Production of Liquid and Gaseous Biofuels*; Academic Press: Cambridge, MA, USA, 2019; pp. 217–244. [CrossRef]

8. Bielecki, M.; Zubkova, V.; Strojwas, A. Influence of Densification on the Pyrolytic Behavior of Agricultural Biomass Waste and the Characteristics of Pyrolysis Products. *Energies* **2022**, *15*, 4257. [CrossRef]
9. Crowley, M.F.; Seiser, R.; Posada, M.A.S.; Maya, J.C.; Chejne, F.; Sitaraman, H.; Usseglio-Viretta, F.; Starace, A.K.; Ciesielski, P.N. Quantifying Impacts of Biomass Pelletization on Fast Pyrolysis Using a Single-Particle Reactor, X-Ray Computed Tomography, and Computational Modeling. *Energy Fuels* **2025**, *40*, 3136–3158. [CrossRef] [PubMed]
10. Abdul-Rahman, A.A.; Yusoff, N.; Abd-Rahman, A. The Effects of Biomass Binders and Moisture Content on the Mechanical Durability of Rice Husk Pellets. *IOP Conf. Ser. Mater. Sci. Eng.* **2020**, *736*, 052013. [CrossRef]
11. Sykorova, V.; Jezerska, L.; Sassmanova, V.; Honus, S.; Peikertova, P.; Kielar, J.; Zidek, M. Biomass Pellets with Organic Binders—Before and after Torrefaction. *Renew. Energy* **2024**, *221*, 119771. [CrossRef]
12. Wang, W.; Lemaire, R.; Bensakhria, A.; Luart, D. Review on the Catalytic Effects of Alkali and Alkaline Earth Metals (AAEMs) Including Sodium, Potassium, Calcium and Magnesium on the Pyrolysis of Lignocellulosic Biomass and on the Co-Pyrolysis of Coal with Biomass. *J. Anal. Appl. Pyrolysis* **2022**, *163*, 105479. [CrossRef]
13. Lazdovica, K.; Liepina, L.; Kampars, V. Catalytic Pyrolysis of Wheat Bran for Hydrocarbons Production in the Presence of Zeolites and Noble-Metals by Using TGA-FTIR Method. *Bioresour. Technol.* **2016**, *207*, 126–133. [CrossRef] [PubMed]
14. Lyu, G.; Wu, S.; Zhang, H. Estimation and Comparison of Bio-Oil Components from Different Pyrolysis Conditions. *Front. Energy Res.* **2015**, *3*, 28. [CrossRef]
15. Nasir Uddin, M.; Daud, W.M.A.W.; Abbas, H.F. Potential Hydrogen and Non-Condensable Gases Production from Biomass Pyrolysis: Insights into the Process Variables. *Renew. Sustain. Energy Rev.* **2013**, *27*, 204–224. [CrossRef]
16. Zhang, Y.; Liang, Y.; Li, S.; Yuan, Y.; Zhang, D.; Wu, Y.; Xie, H.; Brindhadevi, K.; Pugazhendhi, A.; Xia, C. A Review of Biomass Pyrolysis Gas: Forming Mechanisms, Influencing Parameters, and Product Application Upgrades. *Fuel* **2023**, *347*, 128461. [CrossRef]
17. Vilas-Boas, A.C.M.; Tarelho, L.A.C.; Moura, J.M.O.; Gomes, H.G.M.F.; Marques, C.C.; Pio, D.T.; Nunes, M.I.S.; Silvestre, A.J.D. Methodologies for Bio-Oil Characterization from Biomass Pyrolysis: A Review Focused on GC-MS. *J. Anal. Appl. Pyrolysis* **2025**, *185*, 106850. [CrossRef]
18. *LVS EN ISO 712:2011*; Cereals and Cereal Products—Determination of Moisture Content—Reference Method (ISO 712:2009). Latvian Standard (LVS): Riga, Latvia, 2011.
19. Lazdovica, K.; Kampars, V.; Grabis, J. Effect of Zinc-Containing Nanopowders on the Catalytic Intermediate Pyrolysis of Buckwheat Straw by Using TGA-FTIR Method. *J. Anal. Appl. Pyrolysis* **2020**, *152*, 104882. [CrossRef]
20. Sluiter, A.; Hames, B.; Ruiz, R.; Scarlata, C.; Sluiter, J.; Templeton, D.; Crocker, D. *Determination of Structural Carbohydrates and Lignin in Biomass: Laboratory Analytical Procedure (LAP)*; National Renewable Energy Laboratory: Golden, CO, USA, 2008.
21. *CEN/TS 15104:2005*; Solid Biofuels—Determination of Total Content of Carbon, Hydrogen and Nitrogen—Instrumental Methods. European Committee for Standardization (CEN): Brussels, Belgium, 2005.
22. *CEN/TS 15289:2006*; Solid Biofuels—Determination of Total Content of Sulphur and Chlorine. European Committee for Standardization (CEN): Brussels, Belgium, 2006.
23. Miroshnichenko, D.; Koval, V.; Zhylina, M.; Vytrykush, N.; Shved, M.; Miroshnychenko, M.; Omelianchuk, H.; Pyshyev, S. Prediction of Higher Heating Value of Raw Materials and Biochar. *Chem. Chem. Technol.* **2025**, *19*, 354–368. [CrossRef]
24. Zhylina, M.; Shishkin, A.; Miroshnichenko, D.; Sterna, V.; Ozolins, J.; Ansone-Bertina, L.; Klavins, M.; Goel, G.; Goel, S. Granulation and Pyrolysis of Agricultural Residues for an Enhanced Circular Economy. *Results Eng.* **2025**, *26*, 104919. [CrossRef]
25. Zhylina, M.; Karnozhytskyi, P.P.; Miroshnichenko, D.; Konohrai, V.; Sterna, V.; Ozolins, J. The Effect of Growth Stimulants Based on Humic Acids from Ukrainian Lignite and Biochar from Agricultural Residues on the Growth and Development of Lettuce (*Lactuca sativa*). *Agron. Res.* **2025**, *23*, 571–584. [CrossRef]
26. Zhylina, M.; Miroshnichenko, D.; Melnykov, A.; Stepanova, V.; Lazdovica, K.; Zemcenkovs, V.; Sterna, V.; Ozolins, J. Biochar structure development during slow pyrolysis of pellets from barley straw and bran. *Sci. Rep.* **2025**, *15*, 42624. [CrossRef] [PubMed]
27. Lazdovica, K.; Kampars, V.; Liepina, L.; Vilka, M. Comparative Study on Thermal Pyrolysis of Buckwheat and Wheat Straws by Using TGA-FTIR and Py-GC/MS Methods. *J. Anal. Appl. Pyrolysis* **2017**, *124*, 1–15. [CrossRef]
28. Hu, J.; Jiang, B.; Liu, J.; Sun, Y.; Jiang, X. Influence of Interactions between Biomass Components on Physicochemical Characteristics of Char. *J. Anal. Appl. Pyrolysis* **2019**, *144*, 104704. [CrossRef]
29. *ISO 5984:2022*; Animal Feeding Stuffs—Determination of Crude Ash. International Organization for Standardization (ISO): Geneva, Switzerland, 2022.
30. Zong, P.; Jiang, Y.; Tian, Y.; Li, J.; Yuan, M.; Ji, Y.; Chen, M.; Li, D.; Qiao, Y. Pyrolysis Behavior and Product Distributions of Biomass Six Group Components: Starch, Cellulose, Hemicellulose, Lignin, Protein and Oil. *Energy Convers. Manag.* **2020**, *216*, 112777. [CrossRef]
31. Prückler, M.; Siebenhandl-Ehn, S.; Apprich, S.; Höltinger, S.; Haas, C.; Schmid, E.; Kneifel, W. Wheat Bran-Based Biorefinery 1: Composition of Wheat Bran and Strategies of Functionalization. *LWT-Food Sci. Technol.* **2014**, *56*, 211–221. [CrossRef]

32. Li, Y.; Zhao, H.; Sui, X.; Wang, X.; Ji, H. Studies on Individual Pyrolysis and Co-Pyrolysis of Peat–Biomass Blends: Thermal Decomposition Behavior, Possible Synergism, Product Characteristic Evaluations and Kinetics. *Fuel* **2022**, *310*, 122280. [CrossRef]
33. Erić, A.; Cvetinović, D.; Milutinović, N.; Škobalj, P.; Bakić, V. Combined Parametric Modelling of Biomass Devolatilisation Process. *Renew. Energy* **2022**, *193*, 13–22. [CrossRef]
34. Sutcu, H. Pyrolysis of Peat: Product Yield and Characterization. *Korean J. Chem. Eng.* **2007**, *24*, 736–741. [CrossRef]
35. Miroshnichenko, D.; Zhylina, M.; Shmeltser, K. Modern Use of Biochar in Various Technologies and Industries. A review. *Chem. Chem. Technol.* **2024**, *18*, 232–243. [CrossRef]

Disclaimer/Publisher's Note: The statements, opinions and data contained in all publications are solely those of the individual author(s) and contributor(s) and not of MDPI and/or the editor(s). MDPI and/or the editor(s) disclaim responsibility for any injury to people or property resulting from any ideas, methods, instructions or products referred to in the content.